

Supplementary Information

Molecular screening for solid–solid phase transition by machine learning

Daisuke Takagi,¹ Kazuki Ishizaki,² Toru Asahi,^{1,2} Takuya Taniguchi*³

¹ Department of Life Science and Medical Bioscience, Graduate School of Advanced Science and Engineering, Waseda University, 3-4-1 Okubo, Shinjuku-ku, Tokyo 169-8555, Japan

² Department of Advanced Science and Engineering, Graduate School of Advanced Science and Engineering, Waseda University, 3-4-1 Okubo, Shinjuku-ku, Tokyo 169-8555, Japan

³ Center for Data Science, Waseda University, 1-6-1 Nishiwaseda, Shinjuku-ku, Tokyo 169-8050, Japan

* Correspondence to takuya.taniguchi@aoni.waseda.jp

Contents

Supplementary Figures S1-S4 (page 2-5)

Supplementary Tables S1-S5 (page 6-11)

Supplementary References (page 12)

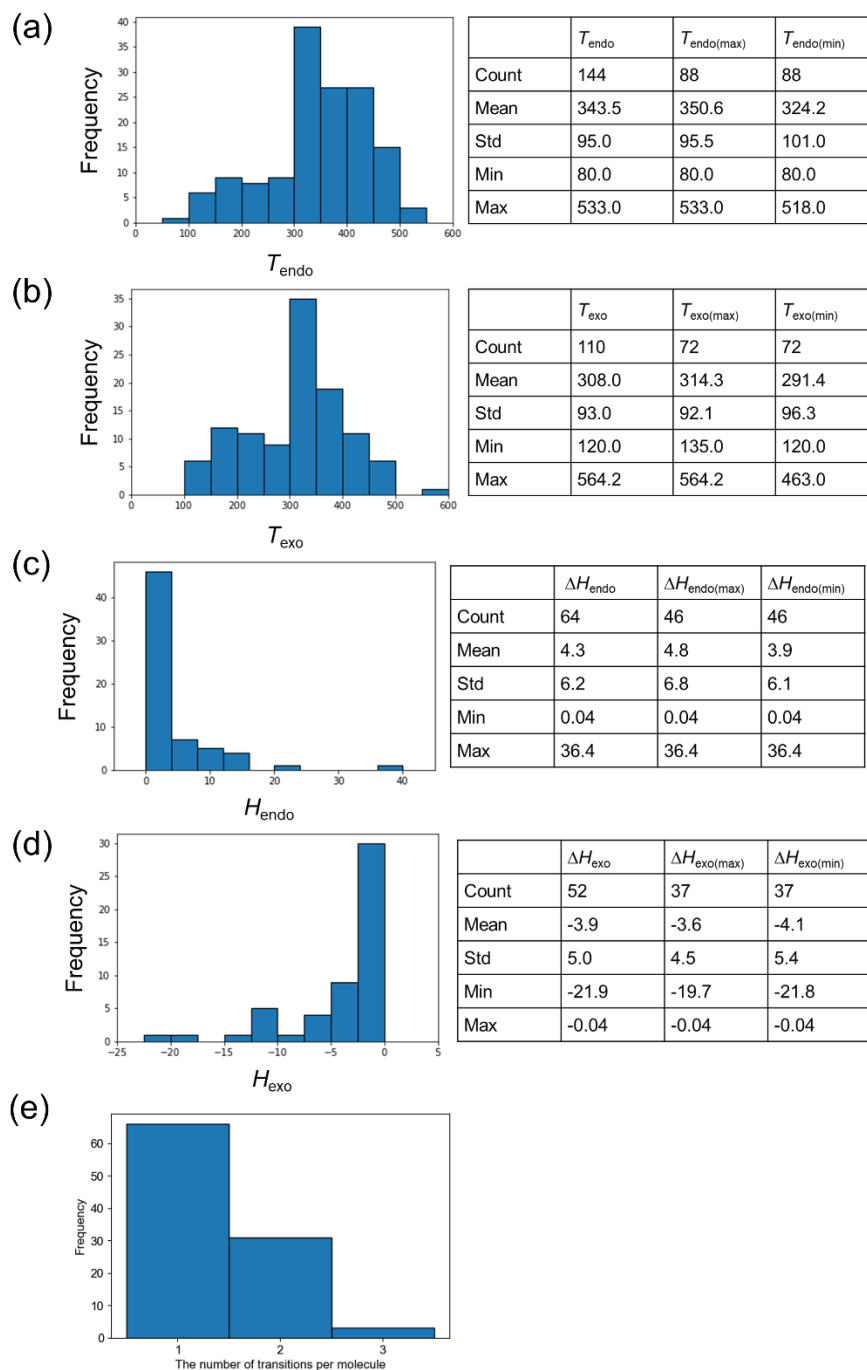


Figure S2. The distribution of positive dataset. (a,b) Statistics of transition temperature corresponding to (a) endothermic and (b) exothermic transitions. (c,d) Statistics of transition enthalpy corresponding to (c) endothermic and (d) exothermic transitions. (e) The distribution of the number of solid phase transitions per molecule.

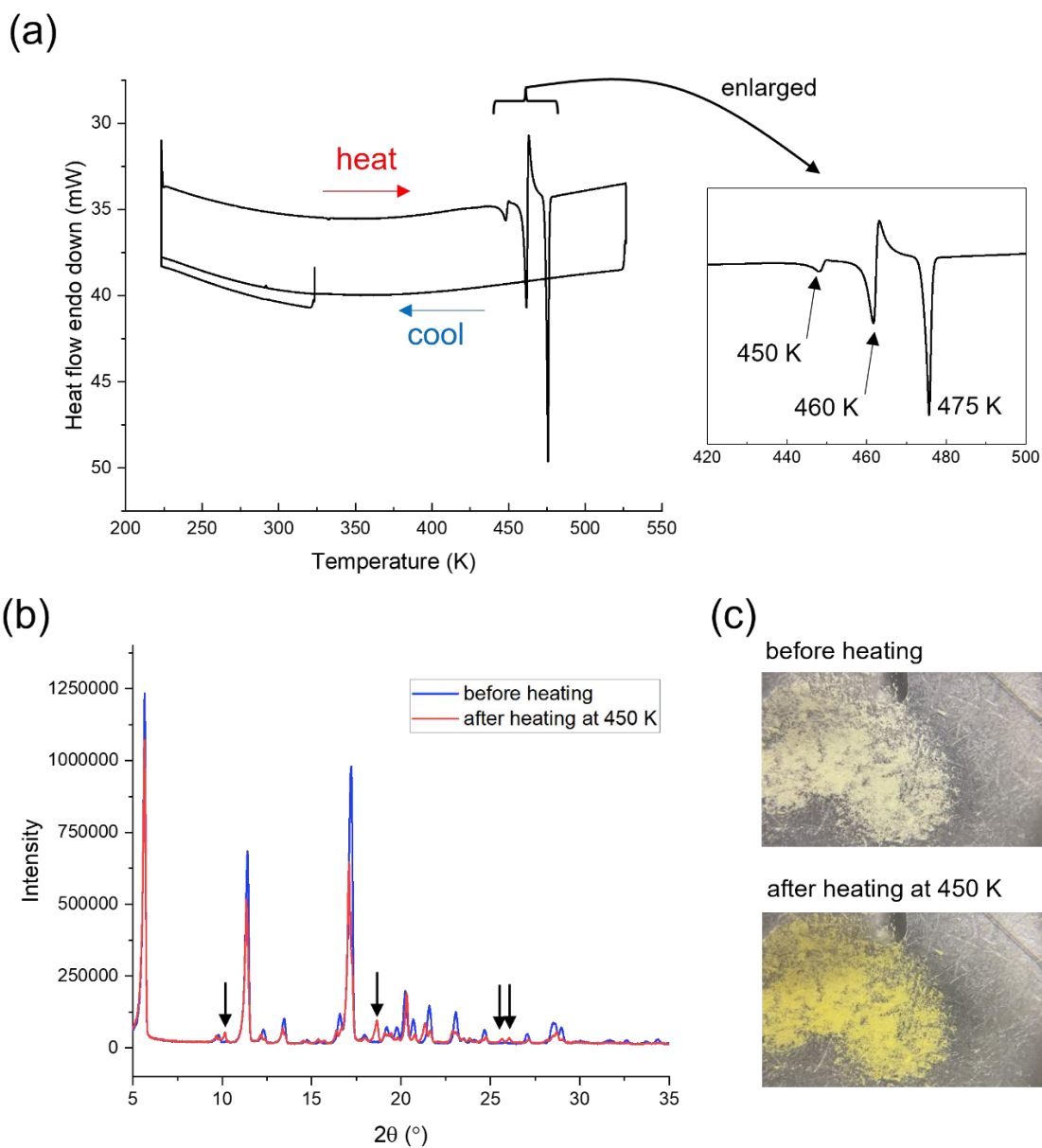


Figure S3. Crystal-to-crystal phase transition of the crystal of OCAPAK. (a) Thermal analysis by DSC. The crystal exhibited a crystal-to-crystal transition at 450 K, and an anomalous endothermic-exothermic peak at 460 K before melting at 475 K. (b) XRD patterns of the crystal before heating, and after heating at 450 K. Both measurements were performed at 293 K. Unique peaks after heating are indicated by arrows. The slight difference of XRD pattern before and after heating reflects the crystal-to-crystal phase transition. (c) Pictures of crystalline powder before and after heating. Crystal appearance did not change before and after heating, although slight color change was observed.



Figure S4. Molecular structures suggested by PU learning with $p = 0.2$. References are summarized in supplementary references.

Supplementary Tables

Table S1. Hyperparameters used for ML models in classification and regression.

ML models	Hyperparameters
Classification	
RF	n_estimators:100, max_depth: None
NN	hidden_layer_sizes: (50,), activation: 'relu'
SVM	kernel: 'rbf', gamma: 0.2
GBDT	n_estimators:100, max_depth: 3
Regression	
NN	hidden_layer_sizes: (100,), activation: 'relu'
RF	n_estimators: 100, max_depth: None
TL-NN	(Search space) n_layers: {1, 10}, n_dim: {50, 100, 200, 300, 400, 500, 750, 1000}
ECFP	n_layers: 5, n_dim: 1000
Avalon	n_layers: 4, n_dim: 750
ErG	n_layers: 3, n_dim: 1000
MACCSKeys	n_layers: 4, n_dim: 1000
Estate	n_layers: 7, n_dim: 1000

Table S2. Comparison of true positive rate (TPR) between PU and BC. The value is the averaged TPR in 10-fold CV.

	PU				BC			
	RF	NN	SVM	GBDT	RF	NN	SVM	GBDT
Mordred	0.13	0.0	0.30	0.96	0.06	0.0	0.0	0.02
ECFP	0.22	0.27	0.39	0.62	0.14	0.13	0.01	0.06
Avalon	0.28	0.21	0.52	0.28	0.14	0.19	0.0	0.01
ErG	0.26	0.21	0.05	0.46	0.12	0.11	0.0	0.0
RDKit	0.20	0.01	0.0	0.74	0.06	0.0	0.0	0.01
MACCSKeys	0.15	0.21	0.20	0.04	0.10	0.14	0.0	0.0
Estate	0.16	0.03	0.0	0.14	0.10	0.0	0.0	0.0

Table S3. Comparison of TPR and SE between each combination of molecular descriptor and classification model. Each value is the average obtained from 10-fold CV.

	TPR				SE			
	RF	NN	SVM	GBDT	RF	NN	SVM	GBDT
Mordred	0.13	0.0	0.30	0.96	69.2	4936.1	1.0	1.0
ECFP	0.22	0.27	0.39	0.62	87.8	1110.4	12441.4	2.1
Avalon	0.28	0.21	0.52	0.28	90.6	2011.0	21990.2	113.3
ErG	0.26	0.21	0.05	0.46	72.9	384.8	64422.4	73.3
RDKit	0.20	0.01	0.0	0.74	248.8	8575.1	NaN*	1.0
MACCSKeys	0.15	0.21	0.20	0.04	67.0	333.7	13594.6	145.3
Estate	0.16	0.03	0.0	0.14	74.0	202.2	171825.4	111.6

* SE was not able to be calculated because n_{up} was zero in the combination of RDKit-SVM.

Table S4. Regression performance based on MAE when using molecular descriptors for each property. Each MAE value represents the mean and standard deviation on five 5-fold CVs. The letter “-“ in TL-NN means the transfer wasn’t succeeded due to the mismatch of input dimension. TL-NN is the best model among all the fine-tuning models.

	NN	TL-NN	RF	mean
<i>T</i> _{endo(max)} (K)				
Mordred	2.0×10 ⁷ (2.4×10 ⁷)	-	58.7 (8.1)	75.4
ECFP	227.8 (21.1)	76.7 (15.8)	71.6 (9.9)	75.4
Avalon	157.1 (25.0)	76.2 (11.8)	64.1 (12.5)	75.4
ErG	206.8 (19.4)	94.1 (21.7)	66.0 (13.2)	75.4
RDkitDesc	149.1 (34.4)	-	70.6 (13.1)	75.4
MACCSKeys	183.9 (29.9)	77.9 (10.6)	69.5 (14.3)	75.4
Estate	220.4 (25.3)	98.2 (20.5)	69.9 (11.7)	75.4
<i>T</i> _{endo(min)} (K)				
Mordred	2.4×10 ⁷ (3.1×10 ⁷)	-	64.9 (9.0)	80.3
ECFP	200.2 (24.7)	75.3 (9.8)	69.8 (14.3)	80.3
Avalon	143.1 (19.8)	75.2 (17.0)	71.3 (14.4)	80.3
ErG	188.6 (28.8)	98.9 (24.1)	68.0 (14.2)	80.3
RDkitDesc	147.5 (30.4)	-	71.1 (17.4)	80.3
MACCSKeys	167.9 (26.5)	80.9 (13.0)	69.9 (12.1)	80.3
Estate	197.9 (20.3)	96.3 (18.0)	74.3 (17.5)	80.3
<i>T</i> _{exo(max)} (K)				
Mordred	1.8×10 ⁷ (2.5×10 ⁷)	-	66.2 (14.4)	71.5
ECFP	196.9 (24.9)	78.3 (16.6)	70.5 (14.0)	71.5
Avalon	151.7 (21.0)	76.1 (19.1)	65.0 (16.4)	71.5
ErG	184.1 (31.0)	105.2 (28.0)	65.7 (16.2)	71.5
RDkitDesc	132.6 (43.7)	-	69.8 (17.3)	71.5
MACCSKeys	161.5 (26.1)	81.8 (14.2)	72.9 (11.6)	71.5
Estate	187.4 (27.6)	100.5 (20.1)	69.7 (12.9)	71.5

$T_{\text{exo(min)}} \text{ (K)}$				
Mordred	3.5×10^7 (3.7×10^7)	-	69.4 (12.8)	80.8
ECFP	173.0 (22.7)	76.2 (16.2)	70.8 (13.7)	80.8
Avalon	137.4 (22.3)	73.5 (16.8)	71.7 (16.1)	80.8
ErG	167.4 (30.2)	99.1 (22.7)	67.4 (13.9)	80.8
RDkitDesc	122.3 (37.2)	-	73.9 (11.2)	80.8
MACCSKeys	145.6 (25.0)	81.1 (16.4)	72.5 (11.8)	80.8
Estate	165.7 (24.5)	93.5 (22.3)	78.5 (16.3)	80.8
$\Delta H_{\text{endo(max)}} \text{ (kJ/mol)}$				
Mordred	2.4×10^7 (4.2×10^7)	-	5.3 (1.3)	4.6
ECFP	4.8 (1.7)	4.8 (2.1)	4.2 (1.4)	4.6
Avalon	4.3 (2.0)	4.8 (2.3)	5.3 (1.4)	4.6
ErG	5.8 (1.4)	4.7 (2.1)	4.5 (1.3)	4.6
RDkitDesc	10.1 (9.5)	-	5.2 (1.5)	4.6
MACCSKeys	4.8 (1.2)	4.7 (2.6)	4.6 (1.4)	4.6
Estate	5.9 (1.8)	4.8 (1.8)	4.4 (1.3)	4.6
$\Delta H_{\text{endo(min)}} \text{ (kJ/mol)}$				
Mordred	1.9×10^7 (2.3×10^7)	-	5.1 (1.3)	3.7
ECFP	4.3 (1.5)	3.9 (1.9)	4.5 (1.8)	3.7
Avalon	4.0 (1.3)	3.9 (1.6)	4.9 (1.4)	3.7
ErG	5.6 (1.9)	3.9 (2.3)	3.8 (1.4)	3.7
RDkitDesc	11.5 (11.1)	-	4.1 (1.2)	3.7
MACCSKeys	4.2 (2.0)	3.9 (2.0)	4.3 (1.7)	3.7
Estate	4.6 (1.3)	4.2 (1.8)	4.0 (1.8)	3.7
$\Delta H_{\text{exo(max)}} \text{ (kJ/mol)}$				
Mordred	1.2×10^7 (1.9×10^7)	-	3.7 (1.0)	3.2
ECFP	3.8 (0.8)	3.5 (1.6)	3.1 (1.2)	3.2
Avalon	3.3 (1.1)	3.5 (1.5)	3.2 (1.1)	3.2
ErG	6.5 (2.2)	3.6 (1.6)	3.5 (1.0)	3.2
RDkitDesc	12.6 (11.5)	-	3.9 (1.2)	3.2
MACCSKeys	4.6 (1.3)	3.5 (1.5)	3.8 (1.0)	3.2
Estate	5.0 (1.6)	3.6 (1.4)	3.7 (0.9)	3.2

$\Delta H_{\text{exo}(\text{min})}$ (kJ/mol)				
Mordred	1.5×10^7 (1.9×10^7)	-	4.3 (1.1)	3.9
ECFP	3.4 (0.9)	4.1 (1.7)	3.4 (1.3)	3.9
Avalon	3.2 (1.0)	4.1 (1.9)	3.3 (1.2)	3.9
ErG	6.4 (1.9)	4.1 (1.8)	3.9 (1.5)	3.9
RDkitDesc	8.7 (3.6)	-	4.3 (1.0)	3.9
MACCSKeys	4.5 (1.1)	4.1 (2.1)	4.5 (1.3)	3.9
Estate	5.1 (2.0)	4.2 (1.2)	4.5 (1.3)	3.9

Table S5. Top-10 ranked important features in the regression of each property. The value in bracket is the averaged value of feature importance.

Rank	$T_{\text{endo(max)}}$	$T_{\text{endo(min)}}$	$T_{\text{exo(max)}}$	$T_{\text{exo(min)}}$
1	VSA_EState4 (0.044)	ATSC2d (0.044)	ATSC1are (0.022)	ATSC1se (0.039)
2	ATSC3p (0.034)	AATS0p (0.036)	VSA_EState4 (0.021)	VSA_EState4 (0.037)
3	ATSC3v (0.031)	VSA_EState4 (0.034)	ATSC5dv (0.020)	ATSC1are (0.036)
4	SLogP_VSA2 (0.031)	JGI1 (0.030)	AATSC3m (0.019)	GATS1d (0.023)
5	ATSC2d (0.018)	AATSC1dv (0.028)	Xc-3d (0.018)	ATSC5d (0.017)
6	AATS0p (0.017)	GATS1p (0.023)	AATSC3Z (0.017)	JGI1 (0.017)
7	GATS3p (0.016)	ATSC3v (0.020)	VSA_Estate3 (0.014)	ATSC1pe (0.017)
8	GATS2d (0.015)	ATSC1se (0.019)	SssssC (0.014)	JGT10 (0.015)
9	Xc-3dv (0.013)	GATS3d (0.017)	Xc-3dv (0.013)	GATS1p (0.015)
10	GATS3v (0.013)	ATSC1pe (0.017)	EState_VSA1 (0.011)	AATSC0d (0.014)

Red bold: the descriptor commonly appeared in $T_{\text{endo(max)}}$, $T_{\text{endo(min)}}$, $T_{\text{exo(max)}}$, and $T_{\text{exo(min)}}$

Black bold: the descriptor commonly appeared in $T_{\text{endo(max)}}$ and $T_{\text{endo(min)}}$

Orange bold: the descriptor commonly appeared in $T_{\text{exo(max)}}$ and $T_{\text{exo(min)}}$

Supplementary references

1. K. Moovendaran and S. Natarajan, *Spectrochim. Acta, Part A*, 2015 **135**, 317-320.
2. P. F. Li, Y. Y. Tang, Z. X. Wang, H. Y. Ye, Y. M. You and R. G. Xiong, *Nat. Commun.*, 2016, **7**, 13635.
3. A. E. Frumkin, N. V. Yudin, K. Y. Suponitsky and A. B. Sheremetev, *Mendeleev Commun.*, 2018, **28**, 135-137.
4. E. Nauha and J. Bernstein, *J. Pharma. Sci.*, 2015, **104**, 2056-2061.
5. A. Lemmerer, *CrystEngComm*, 2012, **14**, 2465-2478.
6. M. Rafilovich, J. Bernstein, M. B. Hickey and M. Tauber, *Cryst. Growth Des.*, 2007, **7**, 1777-1782.
7. C. S. Yang, Y. H. Tan, C. F. Wang, S. P. Chen, B. Wang, H. R. Wen and Y. Z. Tang, *Chem. Phys.*, 2018, **502**, 66-71.
8. T. Kusukawa, Y. Kojima, and F. Kannen, *Chem. Lett.*, 2019, **48**, 1213-1216.
9. C. Liu, J. Chen, C. Xu, H. Hao, B. Xu, D. Hu, G. Shi and Z. Chi, *Dyes Pigm.*, 2020, *174*, 108093.
10. A. Ainurofiq, R. Mauludin, D. Mudhakar, D. Umeda, S. N. Soewandhi, O. D. Putra and E. Yonemochi, *Eur. J. Pharma. Sci.*, 2018, **111**, 65-72.
11. R. Bhowal, A. A. Balaraman, M. Ghosh, S. Dutta, K. K. Dey and D. Chopra, *J. Am. Chem. Soc.*, 2020, **143**, 1024-1037.
12. V. Kumar, R. Thaimattam, S. Dutta, P. Munshi and A. Ramanan, *CrystEngComm*, 2017, **19**, 2914-2924.
13. T. Kojima, F. Kato, R. Teraoka, Y. Matsuda, S. Kitagawa and M. Tsuhako, *Chem. Pharma. Bull.*, 2007, **55**, 407-411.
14. S. Ying, M. Chen, Z. Liu, M. Zheng, H. Zhang, S. Xue and W. Yang, *J. Mater. Chem. C*, 2017, **5**, 5994-5998.
15. A. Kapf, H. Eslahi, M. Blanke, M. Saccone, M. Giese and M. Albrecht, *New J. Chem.*, 2019, **43**, 6361-6371.
16. P. Rani, A. Husain, A. Shukla, N. Singla, A. K. Srivastava, G. Kumar, K. K. Bhasin and G. Kumar, *CrystEngComm*, 2021, **23**, 1859-1869.